THE JOURNAL OF BIOLOGICAL CHEMISTRY VOL. 283, NO. 51, pp. 35638–35643, December 19, 2008

An Intersubunit Hydrogen Bond in the Nicotinic Acetylcholine Receptor That Contributes to Channel Gating*[S]

Received for publication, September 17, 2008, and in revised form, October 21, 2008 Published, JBC Papers in Press, October 24, 2008, DOI 10.1074/jbc.M807226200

Kristin Rule Gleitsman[‡1,2], **Sean M. A. Kedrowski**[‡1,3], **Henry A. Lester**[§], **and Dennis A. Dougherty**[‡4]

From the Divisions of [‡]*Chemistry and Chemical Engineering and* [§]*Biology, California Institute of Technology, Pasadena, California 91125*

The muscle nicotinic acetylcholine receptor is a large, allosteric, ligand-gated ion channel with the subunit composition $\alpha_2\beta\gamma\delta$. Although much is now known about the structure of the binding site, relatively little is understood about how the binding event is communicated to the channel gate, causing the pore to open. Here we identify a key hydrogen bond near the binding site that is involved in the gating pathway. Using mutant cycle analysis with the novel unnatural residue α-hydroxyserine, we find that the backbone N-H of αSer-191 in loop C makes a hydrogen bond to an anionic side chain of the complementary subunit upon agonist binding. However, the anionic partner is not the glutamate predicted by the crystal structures of the homologous acetylcholine-binding protein. Instead, the hydrogen-bonding partner is the extensively researched aspartate γAsp-174/δAsp-180, which had originally been identified as a key binding residue for cationic agonists.

The Cys loop family of ligand-gated ion channels is involved in mediating fast synaptic transmission throughout the central and peripheral nervous systems (1–3). These neuroreceptors are among the molecules of learning, memory, and sensory perception, and they are implicated in numerous neurological disorders, including Alzheimer disease, Parkinson disease, and schizophrenia. The muscle nicotinic acetylcholine receptor (nAChR)[5] is arguably the best-studied member of the Cys loop family. This heteropentameric receptor is composed of homologous but functionally distinct subunits arranged symmetrically around a central ion-conducting pore with the stoichiometry $\alpha_2\beta\gamma\delta$. The agonist binding sites are located at the interfaces between the $\alpha\gamma$ and $\alpha\delta$ subunits. The binding of two agonist molecules induces a conformational change that leads to the opening of the ion channel.

It is now widely appreciated that a tryptophan residue (αTrp-149) plays a key role in neurotransmitter binding by forming a cation-π interaction with the quaternary ammonium group of acetylcholine (4), a result supported by structural data. However, many other important residues in the immediate vicinity of the binding site have been identified. In a classic experiment on the *Torpedo* nAChR (a close homologue of the muscle subtype), Czajkowski and Karlin (5) concluded that a key aspartate (γAsp-174/δAsp-180) from the complementary binding subunit could come within 9 Å of the agonist binding site. Mutation of this residue severely impacted receptor function, leading to a proposal that the negative charge of this aspartate interacted with the positive charge of the agonist (6, 7). Subsequently, however, both the crystal structure of acetylcholine-binding protein (AChBP, a soluble protein homologous to the extracellular domain of the nAChR) (8) and the 4 Å cryo-electron microscopy structure of *Torpedo* nAChR (9, 10) showed that this residue is positioned quite far from the agonist binding site (Fig. 1). Single-channel studies suggest that this residue is primarily important for ligand-induced channel gating rather than agonist binding (11, 12).

γAsp-174/δAsp-180 is part of loop F, the most remote of the six loops originally proposed by Changeux and co-workers (1) to contribute to the agonist binding site. In the carbamylcholine-bound AChBP structure (13), a different F loop anionic residue, γGlu-176/δGlu-182 (AChBP Glu-163), is positioned near loop C of the agonist binding site (Fig. 1). Specifically, γGlu-176/δGlu-182 is within hydrogen-bonding distance of the backbone N-H at αSer-191, which is located on the C loop between the aromatic binding box residue αTyr-190 and the vicinal disulfide formed by αCys-192 and αCys-193. Loop F is generally disordered in the AChBP and nAChR structures, and hydrogen-deuterium exchange mass spectrometry on AChBP reveals that loop F and loop C are the most conformationally dynamic segments of the protein (14). It is generally accepted that agonist binding draws loop C inward, capping the aromatic binding pocket (13, 15). In contrast, crystal structures of AChBP with antagonists bound reveal that loop C pulled away from the agonist binding site (15). Distinctions between antagonist- and agonist-induced motion have also been observed in loop F (16). As such, many investigators favor a gating model involving a contraction of the agonist binding site around an agonist molecule that is largely mediated by movements in loops C and F, although little is known about the nature of the specific interactions involved in this systolic motion.

* This work was supported, in whole or in part, by National Institutes of Health Grants NS 34407 and NS 11756. The costs of publication of this article were defrayed in part by the payment of page charges. This article must therefore be hereby marked "*advertisement*" in accordance with 18 U.S.C. Section 1734 solely to indicate this fact.

[S] The on-line version of this article (available at http://www.jbc.org) contains supplemental text, a supplemental table, and a supplemental figure.

[1] These authors contributed equally to this work.

[2] Partially supported by a National Science Foundation graduate research fellowship.

[3] Partially supported by a National Research Service Award training grant.

[4] To whom correspondence should be addressed: Division of Chemistry and Chemical Engineering, California Institute of Technology, 1200 E. California Blvd., Pasadena, CA 91125. Tel.: 626-395-6089; Fax: 626-564-9297; E-mail: dadougherty@caltech.edu.

[5] The abbreviations used are: nAChR, nicotinic acetylcholine receptor; AChBP, acetylcholine-binding protein; Sah, α-hydroxyserine; Aah, α-hydroxyalanine; Nha, nitrohomoalanine; Akp, 2-amino-4-ketopentanoic acid.

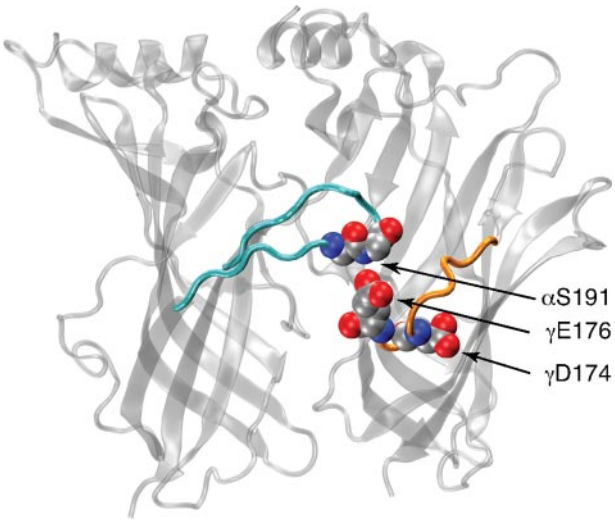

FIGURE 1. **Structure of AChBP with carbamylcholine bound (Protein Data Bank: 1UV6); numbering as in nAChR.** Residues considered here are shown in space filling. The C loop (*cyan*) and F loop (*orange*) are highlighted. In this structure, the C and F loops have closed around the bound agonist (agonist not shown). A carboxylate oxygen (*red*) of γGlu-176 is within hydrogen-bonding distance of the backbone NH (*blue*) of αSer-191.

In the present work, we evaluate several anionic residues in loop F and potential interactions with loop C. Using a combination of natural and unnatural mutagenesis, we find that, indeed, the backbone N-H of αSer-191 does make a hydrogen bond to a loop F residue. However, the partner is not the glutamate seen in the AChBP crystal structure. Instead, the aspartate (γAsp-174/δAsp-180) originally identified by Czajkowski and Karlin (5) is the hydrogen-bonding partner.

EXPERIMENTAL PROCEDURES

Preparation of Unnatural Amino and Hydroxy Acids—All chemical reactions were performed under argon using solvent-column dry solvents (17). Flasks and vials were oven-dried at 122 °C and cooled in a desiccator box containing anhydrous calcium sulfate. Silica chromatography was carried out in accordance with the methods of Still *et al.* (18). The preparations of nitrohomoalanine (Nha), 2-amino-4-ketopentanoic acid (Akp), and α-hydroxyalanine (Aah) have been described previously (19–21).

Synthesis of 2,3-Dihydroxypropionate (α-Hydroxyserine, Sah)-tRNA—Glycerate calcium salt dihydrate (286 mg, 2.0 mmol) were measured into a 100-ml round-bottomed flask. Methanol (40 ml) and toluene (10 ml) were added, followed by concentrated hydrochloric acid (1 ml, 12 mmol). The mixture was stirred under reflux for 6 h, at which point the solvent was removed *in vacuo*. This crude residue was then dissolved in dimethylfomamide (6 ml) in a 2-dram vial. *tert*-Butyldimethylsilyl chloride (906 mg, 6 mmol) and imidazole (544 mg, 8 mmol) were then added, and the reaction was stirred at room temperature for 12 h, at which point the reaction was concentrated *in vacuo* to ~1 ml, and dichloromethane (10 ml) was added. The precipitate was removed by filtration, and the filtrate was reduced *in vacuo* and purified by flash chromatography on silica (5% ethyl acetate in hexanes) to yield 421 mg (60% over two steps) of 2,3-di-(*tert*-butyldimethylsilyl)glycerate methyl ester. ^{1}H NMR (300 MHz, $CDCl_3$) δ 4.27 (dd, 1H, J = 5.2, 6.2 Hz), 3.80 (dd, 1H, J_{AB} = 9.9 Hz, J_{AX} = 5.2 Hz), 3.73 (dd, 1H, J_{AB} = 9.9 Hz, J_{AX} = 6.6 Hz), 3.70 (s, 3H), 0.88 (s, 9H), 0.85 (s, 9H), 0.07 (s, 3H), 0.05 (s, 3H), 0.03 (s, 3H), 0.02 (s, 3H). ^{13}C NMR (75 MHz, $CDCl_3$) δ 172.71, 74.21, 66.16, 51.99, 26.04, 25.94, 18.57, 18.52, −4.86, −4.87, −5.16, −5.25. Low resolution mass spectrometry (ES^+) calculated for $C_{16}H_{36}NaO_4Si_2$ ($[M+Na]^+$) 371.2, found 371.1.

2,3-di-*tert*-(Butyldimethylsilyl)glycerate methyl ester (100 mg, 0.29 mmol) was measured into a 2-dram vial. Diethyl ether (3 ml) was added to dissolve the starting material, followed by potassium trimethylsilanolate (22) (40.7 mg, 0.29 mmol). After 18 h, the potassium salt was isolated by filtration, washed with 2 × 1 ml ether, and dried *in vacuo*. The solid was then resuspended in chloroacetonitrile (3 ml) and allowed to stir at room temperature for 6 h. The reaction was then filtered through a plug of silica to yield the pure product as a colorless liquid: 66.7 mg (62% over two steps) of 2,3-di-*tert*-(butyldimethylsilyl)glycerate cyanomethyl ester. ^{1}H NMR (300 MHz, $CDCl_3$) δ 4.75 (s, 2H), 4.35 (t, 1H, J = 5.4 Hz), 3.81 (d, 2H, J = 5.4 Hz), 0.90 (s, 9H), 0.87 (s, 9H), 0.10 (s, 3H), 0.08 (s, 3H), 0.06 (s, 3H), 0.05 (s, 3H). ^{13}C NMR (75 MHz, $CDCl_3$) δ 170.82, 114.24, 73.78, 65.92, 48.62, 26.01, 25.87, 18.48, −4.86, −4.90, −5.21, −5.24. High resolution mass spectrometry (FAB^+) calculated for $C_{17}H_{36}NO_4Si_2$ ($[M+H]^+$) 374.2183, found 374.2181. The transesterification and deprotection of 2,3-di-*tert*-butyldimethylsilylglycerate cyanomethyl ester were performed according to published protocols to yield Sah-tRNA (23).

Side Chain and Backbone Mutagenesis—Conventional mutagenesis and unnatural mutagenesis, with the site of interest mutated to either an amber stop codon or a four-base frameshift codon (at αSer-191), were achieved by a standard Stratagene QuikChange protocol. Sequencing through both strands confirmed the presence of the desired mutation. Mouse muscle embryonic nAChR in the pAMV vector was used. All the mutations were made in the presence of a background transmembrane mutation (βL9′S) that lowers whole-cell EC_{50} (24, 25). In addition, the α-subunits contain a hemagglutinin epitope in the M3-M4 cytoplasmic loop for Western blot studies. Control experiments show that this epitope does not detectably alter EC_{50}. mRNA was prepared by *in vitro* runoff transcription using the Ambion (Austin, TX) T7 mMessage mMachine kit. For conventional mutants, a total of 2.0–4.0 ng of mRNA was injected in a ratio of 2:1:1:1 of α:β:γ:δ. For suppression with unnatural amino and hydroxy acids, a total of 4.0 ng of mRNA was injected in an α:β:γ:δ subunit ratio of 10:1:1:1. Typically, 25 ng of tRNA was injected per oocyte along with mRNA in a ratio of 1:1 with a total volume of 50 nl/cell. As a negative control for suppression, truncated 74-nucleotide tRNA or truncated tRNA ligated to deoxycytosine adenosine was co-injected with mRNA in the same manner as fully charged tRNA. Data from experiments where currents from these negative controls were greater than 10% of the experimental were excluded. Frameshift suppression at αSer-191 was used for simultaneous incorporation of two unnatural residues (26).

Electrophysiology—The function of mutant receptors was evaluated using two-electrode voltage clamp (see supplemental materials). Stage V–VI oocytes of *Xenopus laevis* were employed. Oocyte recordings were made 12–48 h after injec-

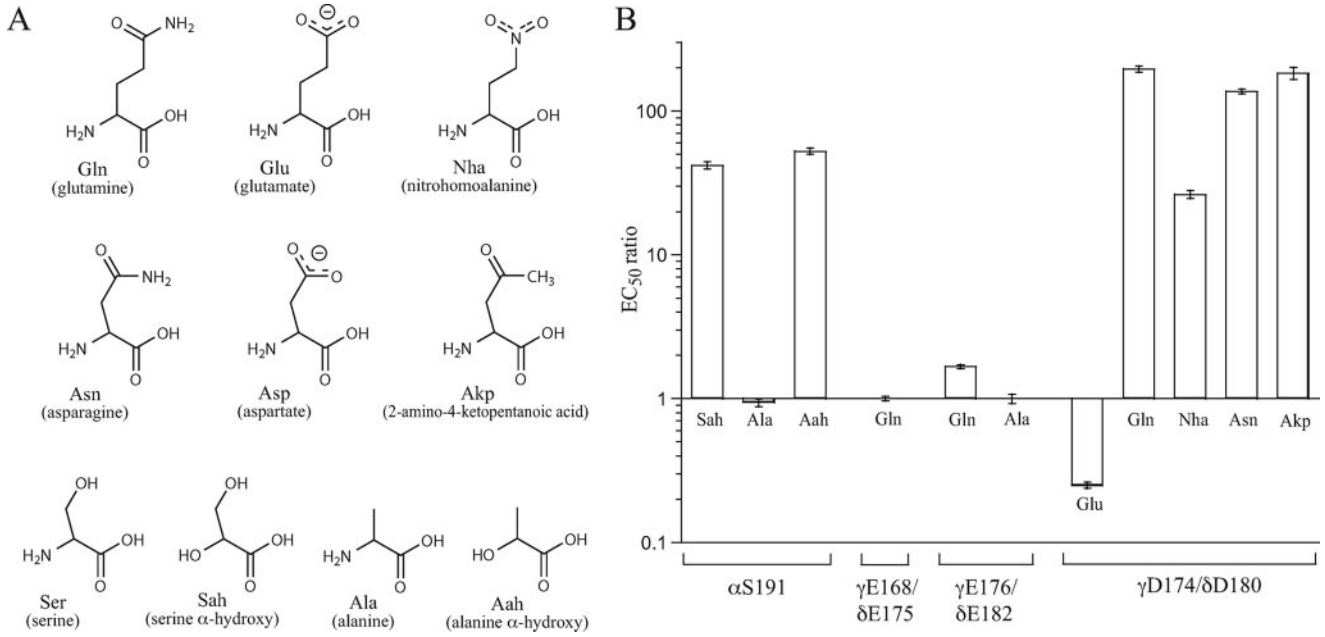

FIGURE 2. *A*, natural and unnatural residues used in this study. *B*, EC_{50} ratios (mutant/wild type) for natural and unnatural substitutions at four sites in the extracellular domain. For glutamine and Nha, EC_{50} ratios were calculated with reference to glutamate instead of wild type (aspartate).

tion in two-electrode voltage clamp mode using the Opus-Xpress 6000A instrument (Axon Instruments, Union City, CA). Oocytes were superfused with a Ca^{2+}-free ND96 solution at flow rates of 1 ml/min before application, 4 ml/min during drug application, and 3 ml/min during wash. Holding potential was −60 mV. Data were sampled at 125 Hz and filtered at 50 Hz. Drug applications were 15 s in duration. Acetylcholine chloride was purchased from Sigma-Aldrich/RBI. Solutions ranging from 0.01 to 5000 μM were prepared in Ca^{2+}-free ND96 from a 1 M stock solution. Dose-response data were obtained for a minimum of eight concentrations of agonists and for a minimum of five cells. Dose-response relations were fitted to the Hill equation to determine EC_{50} and Hill coefficient values. The dose-response relations of individual oocytes were examined and used to determine outliers. The reported EC_{50} values are from the curve fit of the averaged data.

RESULTS

A Backbone Mutation at αSer-191 Has a Large Impact on Receptor Function—In the process of probing the backbone flexibility surrounding the nAChR binding box, we mutated αSer-191 to Sah. This produces an ester backbone linkage at this position, while preserving the side chain. Along with increasing backbone flexibility, this mutation removes the hydrogen bond-donating N-H group and replaces it with a non-hydrogen bond-donating O (Figs. 2 and 3). We have performed similar backbone mutations at several positions throughout the nAChR, and typically, the consequences are not dramatic (19, 27). However, at αSer-191, this subtle mutation leads to a 40-fold increase in EC_{50} (Table 1 and Fig. 2*B*). We also made alanine and Aah mutations at this site. The side chain mutation alone had minimal impact on receptor function, producing no shift in EC_{50}. However, receptor function of the αS191Aah mutant was dramatically impaired relative to αS191Ala, confirming that the backbone, and not the side chain, at αSer-191 is important for receptor function.

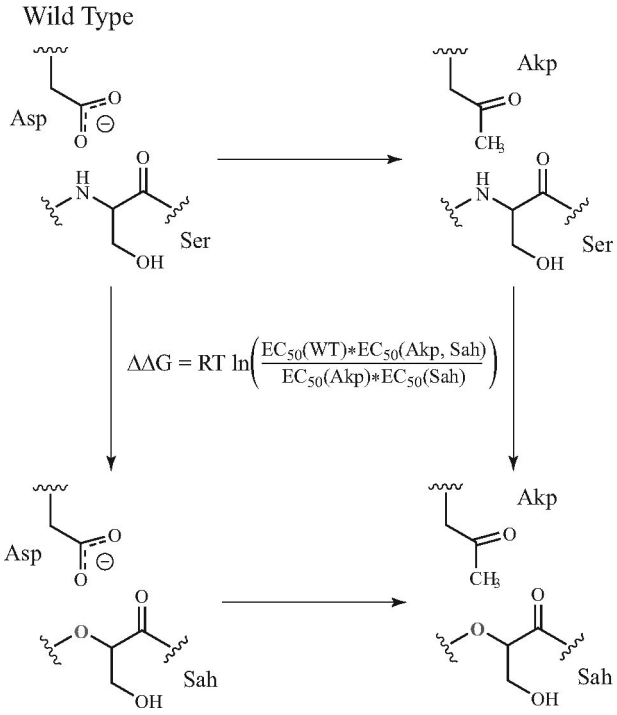

FIGURE 3. **Mutant cycle analysis for a backbone mutation at αSer-191 and a side chain mutation at γAsp-174/δAsp-180 with the equation for calculating the coupling energy.** Note that introducing the α-hydroxy acid Sah removes the backbone NH proposed to hydrogen bond to γAsp-174/δAsp-180.

Evaluating Anionic Residues on Loop F—To evaluate the potential hydrogen bond from αSer-191 to γGlu-176/δGlu-182, we made several mutations at this glutamate. Surprisingly, all mutations have minimal impact, suggesting no critical role for this residue. Another nearby loop F glutamate residue,

TABLE 1

EC_{50} values ± the standard error of the mean for mutations made in this study

In all cases, the β-subunit contains an L9′S mutation.

Mutant	EC_{50}	Double mutant	EC_{50}	$\Delta\Delta G$
	μM		μM	kcal/mol
αβγδ	1.2 ± 0.04			
αS191βγδ Sah	50 ± 2.3			
αβγE176AδE182A	1.2 ± 0.08	αS191Sah/βγE176A/δE182A	32 ± 1.7	0.27 ± 0.06
αβγE176QδE182Q	2.0 ± 0.10	αS191Sah/βγE176Q/δE182Q	51 ± 2.4	0.29 ± 0.03
αβγE168QδE175Q	1.2 ± 0.02	αS191Sah/βγE168Q/δE175Q	37 ± 1.2	0.18 ± 0.05
αβγD174EδD180E	0.3 ± 0.01	αS191Sah/βγD174E/δD180E	15 ± 0.90	0.12 ± 0.05
αβγD174QδD180Q	59 ± 2.0	αS191Sah/βγD174Q/δD180Q	96 ± 5.2	1.9 ± 0.05
αβγD174NhaδD180Nha	7.9 ± 0.40	αS191Sah/βγD174Nha/δD180Nha	31 ± 1.9	1.4 ± 0.05
αβγD174NδD180N	160 ± 2.7	αS191Sah/βγD174Nδ/D180N	190 ± 12	2.1 ± 0.05
αβγD174AkpδD180Akp	220 ± 19	αS191Sah/βγD174Akpδ/D180Akp	190 ± 12	2.3 ± 0.15
αS191βγδ Ala	1.1 ± 0.06	αS191Ala/βγD174Nδ/D180N	230 ± 8.0	0.25 ± 0.04
αS191βγδ Aah	63 ± 2.4	αS191Aah/βγD174Nδ/D180N	130 ± 7.6	2.5 ± 0.04

γGlu-163169/δGlu-163175, was also evaluated. Again, no significant impact was seen.

In sharp contrast, even the subtlest mutations at γAsp-174/δAsp-180 produce large effects upon receptor function, a result that others have also seen (5, 6, 28, 29). We first studied asparagine, glutamate, and glutamine mutations at this site. The γD174E/δD180E mutant exhibits a modest ~3-fold decrease in EC_{50}. However, the γD174N/δD180N and γD174Q/δD180Q mutants produce substantial (>100-fold) changes to the EC_{50} (Fig. 2*B* and Table 1).

Fundamentally, the results of these conventional mutations strongly implicate the side chain of γAsp-174/δAsp-180 in an electrostatic interaction, such as an ion pair or hydrogen bond. However, changing the side chain functionality from a carboxylate to an amide not only neutralizes the charge on the side chain, it also desymmetrizes it and introduces a potential hydrogen bond donor. To better understand the role of γAsp-174/δAsp-180, we incorporated two unnatural amino acids.

Nha is an analogue of glutamate that contains a nitro (NO_2) group, which is isosteric and isoelectronic to a carboxylate, but it has no charge and is a much weaker hydrogen bond acceptor (Fig. 2*A*).[6] Incorporation of Nha at γAsp-174/δAsp-180 yields a slightly less dramatic effect than the γD174N/δD180N and γD174Q/δD180Q mutants, producing a 24-fold shift in EC_{50} relative to γD174E/δD180E (Fig. 2*B*). Thus, charge neutralization at this site significantly affects receptor function but cannot fully account for the EC_{50} shift seen in the γD174N/δD180N and γD174Q/δD180Q mutants.

The second unnatural amino acid analogue incorporated at γAsp-174/δAsp-180 was Akp. Akp is isoelectronic to Asp but possesses a methyl ketone functionality in place of the carboxylate (Fig. 2*A*). As such, Akp is a desymmetrized analogue of Asp, similar to Asn, but it has different electrostatic properties (less polar, weaker hydrogen bond acceptor, and cannot donate a hydrogen bond). When Akp is incorporated at γAsp-174/δAsp-180, its effect upon receptor function is roughly as deleterious as the Asn mutation (Fig. 2*B*). Mutations at individual binding sites (αβγD174Nδ and αβγδD180N) showed substantial (~50-fold) and approximately equivalent increases in whole cell EC_{50} (supplemental Table 1).

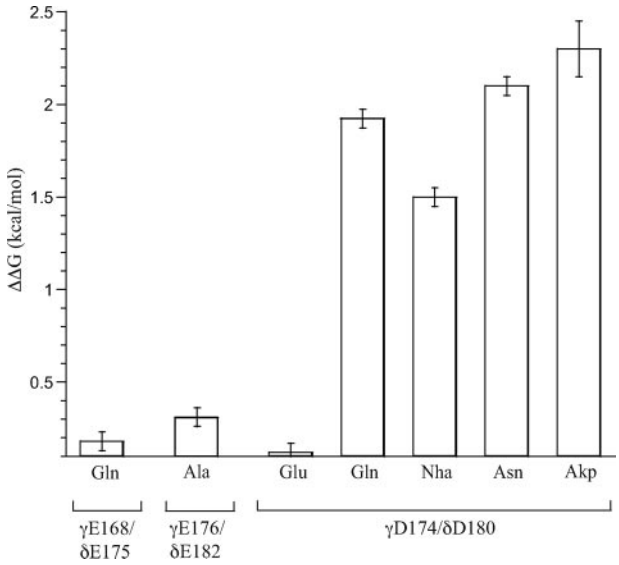

FIGURE 4. **Coupling energies between various side chain mutants in the complementary binding subunit and the backbone mutation at αSer-191 (αS191Sah).** For glutamine and Nha, free energy calculations were made with reference to glutamate instead of wild type (aspartate).

Mutant Cycle Analysis Reveals a Strong Interaction between the αSer-191 Backbone and the Side Chain of γAsp-174/δAsp-180—Mutant cycle analysis was performed between several of the side chain mutations at γAsp-174/δAsp-180 and the αS191Sah mutation (Figs. 3 and 4). Briefly, mutant cycle analysis is used to determine the pairwise interaction energy between two residues in a protein using the equation given in Fig. 3. If the two residues do not interact, the change in free energy for the simultaneous mutation of both residues should simply be the sum of the free energy of each of the individual mutations. However, for residues that interact, the change in free energy for the double mutation will be non-additive. EC_{50}-based mutant cycle analysis has been used to investigate interactions in Cys loop receptors by other researchers (30–32). Further discussion can be found in the supplemental materials.

Lengthening the side chain (γD174E/δD180E) has no impact on the interaction between these two residues ($\Delta\Delta G$ = 0.12 kcal/mol). In contrast, mutant cycle analysis between γD174N/δD180N and αS191Sah indicates a large energetic coupling ($\Delta\Delta G$ = 2.1 kcal/mol). A smaller but still quite significant effect

[6] Although nitroalanine, the analogue of aspartate, would be ideal, it is not chemically compatible with the nonsense suppression methodology. Given that the mutation γD174E/δD180E produces a very modest EC_{50} shift and that γD174N/δD180N and γD174Q/δD180Q show similar effects on receptor function, the comparison of Nha with Glu can be considered meaningful.

is seen for the mutant cycle analysis between γD174Nha/δD180Nha and αS191Sah ($\Delta\Delta G = 1.4$ kcal/mol). Mutant cycle analyses of γD174N/δD180N with αS191A and αS191Aah further support the conclusion that the interaction between these residues involves the backbone of αSer-191 and not the side chain (αS191Ala: $\Delta\Delta G = 0.25$; αS191Aah: $\Delta\Delta G = 2.3$ kcal/mol). Not surprisingly, comparable mutant cycle analyses of the two glutamates of loop F, γGlu-176/δGlu-182 and γGlu-163169/δGlu-163175, with αS191Sah showed no significant coupling.

DISCUSSION

The AChBP crystal structures transformed the study of nAChRs by providing high resolution structural data about the ligand binding domain of these proteins. In addition to refining our existing structural knowledge of the receptor, obtained from decades of careful biochemical research, it served as a valuable starting point for new structure-function studies on the receptor. However, AChBP is not a ligand-gated ion channel and, in fact, shares less than 25% homology with its nearest Cys loop relative, the α7 nAChR (8). As such, some fundamental structural differences must exist between AChBP and actual Cys loop receptors, particularly pertaining to residues involved in mediating communication between the binding site and the ion channel pore.

Arguably the biggest discrepancy between the AChBP structures and prior biochemical studies of the nAChR concerns the loop F residue γAsp-174/δAsp-180. A remarkable cross-linking study in the *Torpedo* nAChR indicated that this residue can come within 9 Å of the vicinal disulfide on the C loop, located at the heart of the agonist binding site (5). However, in AChBP, the residue that aligns with γAsp-174/δAsp-180 is not at all near the agonist binding site. In addition, the cryo-electron microscopy structure of the *Torpedo* nAChR, which is believed to be in the desensitized or closed state, places this residue tucked deeply inside a β-sheet-lined hydrophobic pocket, over 15 Å from loop C (9, 10).

Although γAsp-174/δAsp-180 is remote to the agonist binding site in AChBP, another loop F anionic residue, γGlu-176δGlu-182, appears to make a hydrogen bond to a backbone N-H that is integral to the aromatic box of the agonist binding site when the agonist carbamylcholine is bound. Using nonsense suppression methodology, we have been able to specifically remove the backbone N-H in question by replacing αSer-191 with its α-hydroxy analogue. Consistent with the AChBP images, this subtle structural change has a large effect on receptor function, suggesting that a hydrogen bond to this moiety is important. However, consistent with prior mutational analyses (6, 7, 28), we find that γGlu-176/δGlu-182 does not play a large role in receptor function. This suggests that AChBP does not provide an accurate model of the muscle nAChR in this region. Given that the sequence alignment in this region shows a number of insertions in nAChR relative to AChBP, combined with the fact that the F loop is believed to be involved in gating the nAChR (AChBP does not gate), it is not surprising that AChBP would be an unreliable model here.

Our results indicate that the hydrogen-bonding partner for the backbone N-H of αSer-191 in the nAChR is instead the side chain of γAsp-174/δAsp-180. Based on the available structural and functional data, we suggest that this hydrogen bond exists in the open state only (11, 28, 29). As others have seen, a number of mutations of this side chain profoundly affect receptor function. Here we employ several relatively subtle mutations. The fact that substantial functional consequences are seen suggests a precise structural role for this side chain in at least one state crucial for activating the channel. Furthermore, all mutations at γAsp-174/δAsp-180 that significantly impact function also show strong coupling to the αS191Sah backbone mutation via mutant cycle analysis. The nature of the coupling is as one would expect from the hydrogen-bonding model. Mutation at either site has a strong effect; however, once the αS191Sah mutation is introduced, removing any possible hydrogen-bonding interaction, mutations at γAsp-174/δAsp-180 have a *much* smaller impact. Interestingly, no specific role for the side chain of αSer-191 is found as the αS191A mutant gives essentially wild-type behavior.[7] However, when the alanine side chain is combined with the α-hydroxy backbone mutation, the same coupling to γAsp-174/δAsp-180 is observed.

We propose that the movement of loop F of the complementary subunit from a position remote to the agonist binding site to one of close proximity to loop C of the principal subunit is a key early structural change associated with nAChR gating. Driving this structural reorganization is the formation of a hydrogen bond between the side chain of γAsp-174/δAsp-180 and the backbone N-H of αSer-191. In the closed state of the wild-type receptor, αSer-191 and the C loop project out into solution, away from the bulk of the receptor, whereas γAsp-174/δAsp-180 of the F loop projects deep within a hydrophobic cavity. Although the energetic desolvation penalty of burying a charged residue within a hydrophobic cavity is significant,[8] it alone is apparently not sufficient to overcome other structural elements that bias this conformation of the F loop. However, agonist binding induces a centripetal movement of the C loop, bringing the backbone N-H of αSer-191 in closer proximity to the F loop. This structural change makes possible a hydrogen bond between γAsp-174/δAsp-180 and the C loop backbone. We hypothesize that the formation of this hydrogen bond, along with the energetic solvation benefit of moving γAsp-174/δAsp-180 into an aqueous environment, provides sufficient driving force to move γAsp-174/δAsp-180 out of its pocket, inducing a movement of the F loop toward the C loop.[9] This structural rearrangement of loop F contributes to the gating pathway. Using rate-equilibrium free energy relationships, Auerbach and co-workers (34) have also concluded that γAsp-174/δAsp-180 moves early in the gating process.

Our results provide an explanation for the cross-linking studies of Czajkowski and Karlin (5), and they are not in conflict with available structural information. The cryo-electron microscopy images of the *Torpedo* receptor show greater than 20 Å separation between αSer-191 and γAsp-174/δAsp-180 in

[7] In AChBP structures, the αSer-191 side chain also makes hydrogen bonds to γGlu-176/δGlu-182.

[8] Based on the hydrophobicity constant, π, the expected desolvation penalty for an aspartic acid residue would be on the order of 1 kcal/mol (33).

[9] The possibility of a salt bridge forming here can be eliminated, given that there are no basic residues in the C loop or in its vicinity.

the closed state. Still, the distance of less than 9 Å that is suggested by the cross-linking studies is plausible, provided that the residues are free to move closer, as occurs in our model of channel gating. A comparison of AChBP structures with and without agonist bound likewise shows that motions of loops C and F are the dominant structural rearrangements that occur when agonist binds. The fact that the hydrogen bond acceptor in loop F differs between AChBP and nAChR is not surprising, given that loop F is strongly implicated in nAChR gating and AChBP did not evolve to have a gating function.

This model is also consistent with the γ174/δ180 mutants described here. Lengthening the side chain of this key F loop residue (γD174E/δD180E) effects a modest improvement in receptor function, either because the longer side chain can more easily reach its αSer-191 hydrogen-bonding partner or because it fits more poorly in the hydrophobic pocket, destabilizing the closed state. Any mutation that eliminates side chain charge has a significant impact on function, which is expected, given that these mutant side chains are poorer hydrogen bond acceptors and that they experience a much lower energetic solvation benefit upon moving from the hydrophobic pocket into an aqueous environment.

In conclusion, mutant cycle analysis involving a novel backbone mutant has identified an important interaction between an F loop residue that has long been thought to contribute to receptor function and the peptide backbone of loop C. The hydrogen bond between the side chain of γAsp-174/δAsp-180 and the backbone of αSer-191 likely forms upon agonist binding and is part of the agonist-induced conformational changes that lead to channel opening. Along with contributing new insights into the gating pathway of the nAChR, our results reconcile a long-standing discrepancy between early biochemical studies of the receptor and structural models from the AChBP systems.

REFERENCES

1. Corringer, P. J., Le Novere, N., and Changeux, J. P. (2000) *Annu. Rev. Pharmacol. Toxicol.* **40,** 431–458
2. Grutter, T., and Changeux, J. P. (2001) *Trends Biochem. Sci* **26,** 459–463
3. Karlin, A. (2002) *Nat. Rev. Neurosci.* **3,** 102–114
4. Zhong, W., Gallivan, J. P., Zhang, Y., Li, L., Lester, H. A., and Dougherty, D. A. (1998) *Proc. Natl. Acad. Sci. U. S. A.* **95,** 12088–12093
5. Czajkowski, C., and Karlin, A. (1991) *J. Biol. Chem.* **266,** 22603–22612
6. Czajkowski, C., and Karlin, A. (1995) *J. Biol. Chem.* **270,** 3160–3164
7. Czajkowski, C., Kaufmann, C., and Karlin, A. (1993) *Proc. Natl. Acad. Sci. U. S. A.* **90,** 6285–6289
8. Brejc, K., van Dijk, W. J., Klaassen, R. V., Schuurmans, M., van Der Oost, J., Smit, A. B., and Sixma, T. K. (2001) *Nature* **411,** 269–276
9. Miyazawa, A., Fujiyoshi, Y., Stowell, M., and Unwin, N. (1999) *J. Mol. Biol.* **288,** 765–786
10. Unwin, N. (2005) *J. Mol. Biol.* **346,** 967–989
11. Akk, G., Zhou, M., and Auerbach, A. (1999) *Biophys. J.* **76,** 207–218
12. Sine, S. M., Shen, X. M., Wang, H. L., Ohno, K., Lee, W. Y., Tsujino, A., Brengmann, J., Bren, N., Vajsar, J., and Engel, A. G. (2002) *J. Gen. Physiol.* **120,** 483–496
13. Sixma, T. K., and Smit, A. B. (2003) *Annu. Rev. Biophys. Biomol. Struct.* **32,** 311–334
14. Shi, J., Koeppe, J. R., Komives, E. A., and Taylor, P. (2006) *J. Biol. Chem.* **281,** 12170–12177
15. Hansen, S. B., Sulzenbacher, G., Huxford, T., Marchot, P., Taylor, P., and Bourne, Y. (2005) *EMBO J.* **24,** 3635–3646
16. Hibbs, R. E., Radic, Z., Taylor, P., and Johnson, D. A. (2006) *J. Biol. Chem.* **281,** 39708–39718
17. Pangborn, A. B., Giardello, M. A., Grubbs, R. H., Rosen, R. K., and Timmers, F. J. (1996) *Organometallics* **15,** 1518–1520
18. Still, W. C., Kahn, M., and Mitra, A. (1978) *J. Org. Chem.* **43,** 2923–2925
19. Cashin, A. L., Torrice, M. M., McMenimen, K. A., Lester, H. A., and Dougherty, D. A. (2007) *Biochemistry* **46,** 630–639
20. England, P. M., Lester, H. A., and Dougherty, D. A. (1999) *Tetrahedron Lett.* **40,** 6189–6192
21. Mu, T. (2006) *A Chemical-Scale Study on the Ligand-Binding Site of a Serotonin-Gated Ion Channel*, Ph.D. thesis, California Institute of Technology, Pasadena, CA
22. Laganis, E. D., and Chenard, B. L. (1984) *Tetrahedron Lett.* **25,** 5831–5834
23. Nowak, M. W., Gallivan, J. P., Silverman, S. K., Labarca, C. G., Dougherty, D. A., and Lester, H. A. (1998) *Methods Enzymol.* **293,** 504–529
24. Filatov, G. N., and White, M. M. (1995) *Mol. Pharmacol.* **48,** 379–384
25. Labarca, C., Nowak, M. W., Zhang, H., Tang, L., Deshpande, P., and Lester, H. A. (1995) *Nature* **376,** 514–516
26. Rodriguez, E. A., Lester, H. A., and Dougherty, D. A. (2006) *Proc. Natl. Acad. Sci. U. S. A.* **103,** 8650–8655
27. England, P. M., Zhang, Y., Dougherty, D. A., and Lester, H. A. (1999) *Cell* **96,** 89–98
28. Martin, M., Czajkowski, C., and Karlin, A. (1996) *J. Biol. Chem.* **271,** 13497–13503
29. Martin, M. D., and Karlin, A. (1997) *Biochemistry* **36,** 10742–10750
30. Kash, T. L., Jenkins, A., Kelley, J. C., Trudell, J. R., and Harrison, N. L. (2003) *Nature* **421,** 272–275
31. Price, K. L., Millen, K. S., and Lummis, S. C. (2007) *J. Biol. Chem.* **282,** 25623–25630
32. Venkatachalan, S. P., and Czajkowski, C. (2008) *Proc. Natl. Acad. Sci. U. S. A.*
33. Eisenberg, D., and McLachlan, A. D. (1986) *Nature* **319,** 199–203
34. Grosman, C., Zhou, M., and Auerbach, A. (2000) *Nature* **403,** 773–776